Design and Characterization Concepts of a Broadband Chip-Integrated Antenna

Martin Hitzler, Christian Waldschmidt
Institute of Microwave Techniques, University of Ulm, 89081 Ulm, Germany
martin.hitzler@uni-ulm.de, christian.waldschmidt@uni-ulm.de

Abstract—**This paper presents the integrated antenna of a frequency modulated constant wave (FMCW) radar chip operating in the 79 GHz band. Besides the transmitting and receiving mode of the chip, an alternative to characterize the antenna reflection coefficient, gain, and radiation pattern are implemented on chip. The multiple options are established by using the focused ion beam (FIB) process in combination with a short-circuited quarter wavelength transformer. Additionally, a through-reflect-line (TRL) calibration is provided on chip to deembed the probe tips. The measured 10 dB matching bandwidth of the antenna is 9 GHz with a flat gain of 2 dBi and a radiation efficiency of about 30%.**

Keywords—integrated antenna, on-chip antennas, millimeter-wave antennas, calibration, gain measurement

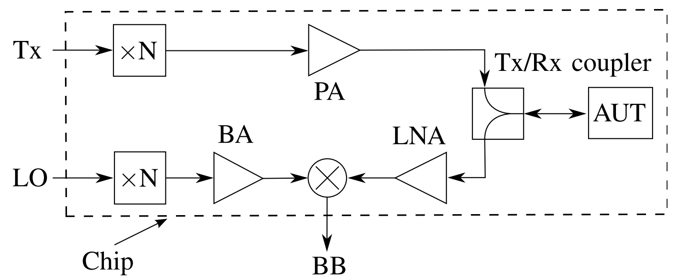

Fig. 1: Schematic view of the FMCW radar.

I. Introduction

The progress of the silicon germanium (SiGe) BiCMOS technology facilitates the integration of complete transceivers in the millimeter wave range and above [1], [2]. A wide range of applications arises at these frequencies like high data rate point-to-point links [3] and short range radars [4] among many others.

Besides the active components the integration of the radiating element is a main challenge of these approaches due to the poor radiation efficiency from a SiGe chip. To overcome this issue, a variety of antenna implementations are given in the literature. The localized backside etching (LBE) process can be used to remove the silicon bulk locally under the silicon dioxide with the metal structures resulting in lower loss components and antennas [5]. Another possible solution are dielectric resonator antennas mounted on top of the chip trying to dislocate the electromagnetic wave of the lossy silicon and silicon dioxide into the dielectric resonator [6].

The approach presented in this paper is based on a superstrate with a patch antenna placed on top of the chip. Investigations on the radiation efficiency of such antennas have been discussed and measured up to 56% in [7]. Comparatively high efficient chip-integrated antennas often exhibit fractional bandwidths under 10% like [8]. A known concept for a superstrate antenna from [9] is adapted to increase the bandwidth above 10%. A probe based measurement setup is provided to verify the simulated antenna gain and matching. This characterization is realized by using the FIB process on a chip being identically constructed as the one working as an FMCW radar.

After a short description of the FMCW radar structure on the chip in Section II, the antenna concept is discussed in Section III. The assembly of the chip and the superstrate into the QFN package is explained in Chapter IV. Finally, the measurement setups and the evaluation are presented in Section V.

II. Composition of the FMCW Radar Chip

The FMCW radar implemented on a chip is depicted in Fig. 1. The frequency modulated transmit (Tx) and local oscillator (LO) signal are generated in a lower frequency band and fed to the chip. The frequency multipliers increase the operating frequency to the desired band around 79 GHz. After the power amplifier (PA) stage, the transmit signal is guided to the transmit / receive (Tx/Rx) coupler. In this monostatic radar the antenna on chip (Antenna Under Test = AUT) radiates the transmit signal and receives the reflected signal from the target. Being reinforced in the low noise amplifier (LNA) the detected signal is down converted with the LO signal at the mixer to baseband (BB). Further signal processing is done off-chip on a printed circuit board (PCB).

III. Antenna Concept

The integrated antenna is based on the design in [9] using a short-circuited $\lambda/4$ patch in the topmost metal layer. On top of the chip a thin dielectric plate is mounted with a common $\lambda/2$ patch antenna representing the actual radiating element. The short-circuited patch on the chip surface is used to couple to the radiating patch as efficient as possible. A 127 µm thin RO3003 substrate from Rogers Corporation [10] was used to have an easily processible substrate material. Besides two additional $\lambda/4$ transformers the nonresonant edge length of the radiating patch on the superstrate was chosen approximately 40% longer than the resonating edge length. Both measures increase the relative 10 dB-bandwidth to finally 15% in the simulation. As a consequence of the large radiating patch antenna the superstrate is projecting above one chip edge resulting in an easy possibility to fix it with a glue dot next to the chip. The

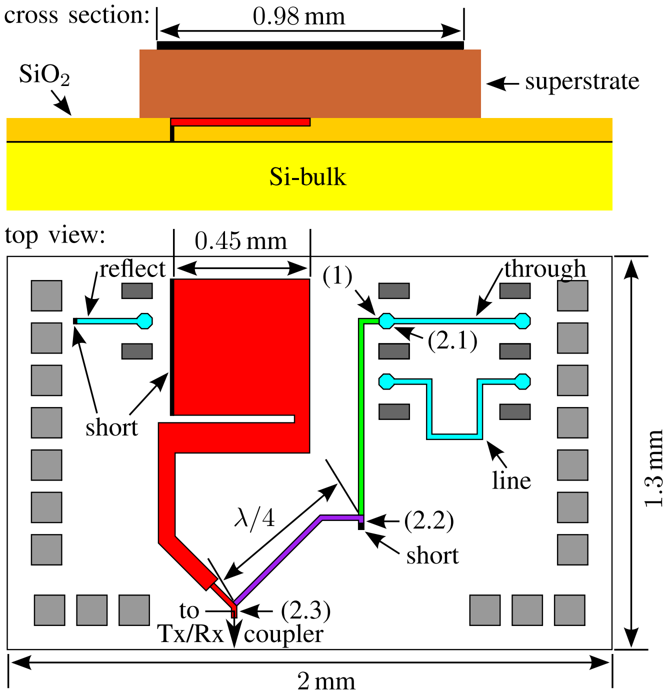

Fig. 2: Schematic of the chip layout with calibration structures.

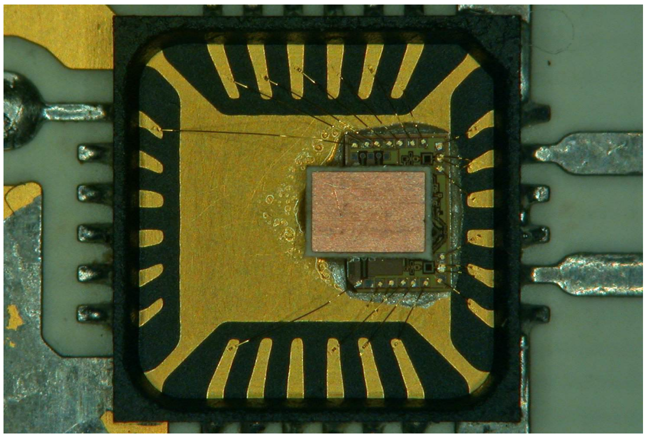

Fig. 3: Packaged chip with superstrate and wire bonds in an open QFN package mounted on a PCB.

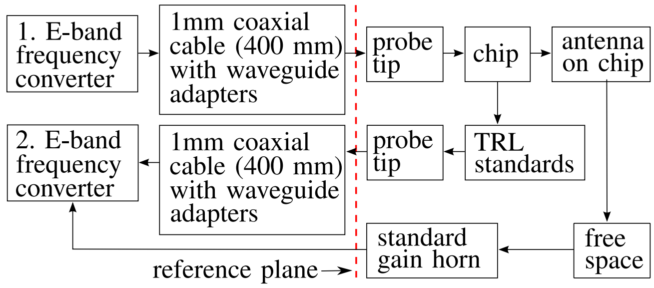

(a) Schematic of the circuitry.

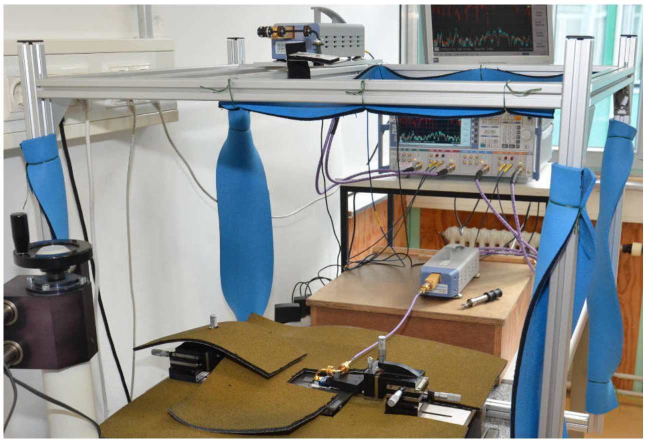

(b) Overview of the measurement setup.

Fig. 4: Antenna characterization at the probe station.

bonds slightly increase the gain to broadside and reduce lateral radiation.

A schematic of the resulting chip layout is presented in Fig. 2 containing the antenna coupling structure (red) with an additional short-circuited $\lambda/4$ transformer (purple) parallel to the antenna structure. Besides the short circuit at the end of the purple line a transmission line in green is connected to this point. It joins the through standard of the on-chip TRL calibration in turquoise with the feeding network of the integrated antenna. For this reason a probe based measurement of the antenna characteristics is possible with the application of the FIB process being further explained in Section V.

IV. Assembly

The bare die was fabricated in the BiCMOS research technology SG13G2 at the IHP [11]. The FIB process was performed on single chips before packaging. An open QFN package with 24 pins was used for housing the 2 mm × 1.3 mm chip to achieve a simple connection to the PCB. Having mounted the chip with conductive silver lacquer on the exposed pad of the QFN package the dielectric plate was fixed with a glue dot of epoxy resin adhesive next to the chip. Bonding the chip pads to the QFN package pins was the last step of the processing and was omitted for the probe based measurements. Due to the comparatively low frequencies at the bond wires a standard bond process could be applied. Figure 3 depicts the assembled chip with the dielectric plate on top in the QFN package.

V. Measurement Setups and Results

The antenna characterization is split into two parts. At first the setup with probe tips was employed to measure the antenna matching and the gain to broadside. In the second part the radiation pattern of the antenna was measured in an anechoic chamber with the packaged chip as a transmitting element.

A. Determination of Antenna Reflection Coefficient and Gain

The starting point for measurements at the probe station was the deembedding of the probe tips with a TRL calibration on chip. The three standards were measured with the arrangement shown in Fig. 4a. The first E-band frequency converter module fed a 1 mm coaxial cable being 40 cm long over a waveguide to coaxial adapter. On the probe station the

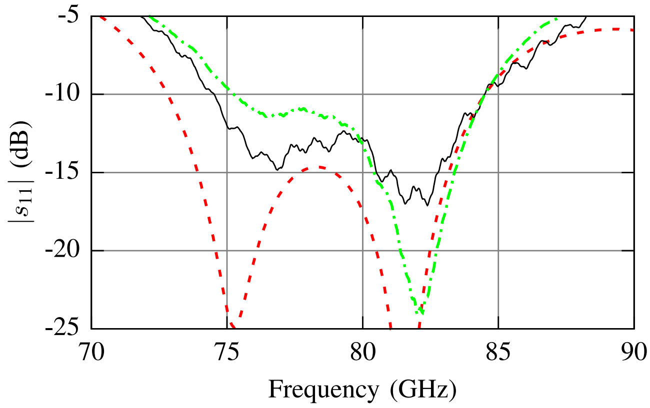

Fig. 5: Simulated (- - -) and measured reflection coefficient of the AUT for a complete TRL calibration to the chip with the network analyzer (- · -) and a deembedded reflection measurement (—).

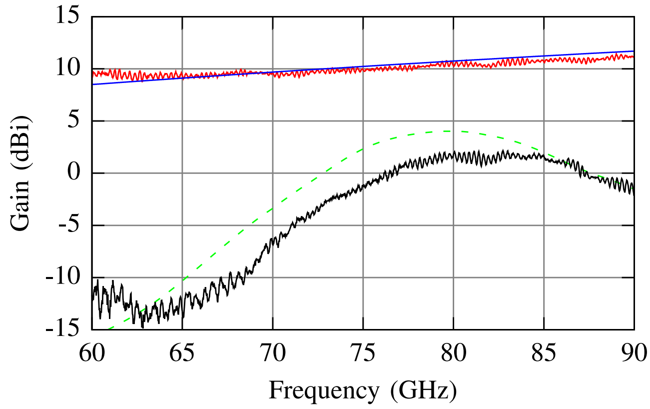

Fig. 6: Simulated (- - -) and measured (—) gain of the AUT and the specified (—) and measured (—) gain of the 10 dBi reference horn antenna to broadside respectively.

coaxial cable was connected to a second adapter reconverting to the rectangular waveguide. The second waveguide port at the probe station was connected in the same manner to the second frequency converter module. A common TRL calibration was performed at these waveguide ports marking the reference plane of the following investigations. Initially, the TRL standards on the chip were recorded to deembed the probe tip transition in the measured curves. For that reason the FIB had to cut through the microstrip line on a test chip at position (1) in Fig. 2 to realize a correct through standard.

The antenna reflection coefficient could be measured after machining the chip with the AUT at positions (2.1), (2.2), and (2.3) in Fig. 2 with the FIB. Position (2.1) means cutting off the lateral area of the pad to create a more homogeneous cross section along the microstrip line.

The simulated and deembedded reflection coefficients of the integrated antenna are depicted in Fig. 5 for two measurement scenarios. The curve of the on-chip TRL calibration with the network analyzer shows less ripple than the deembedded curve. Both measured reflection coefficients are slightly shifted by about 1 GHz to upper frequencies. A source for the frequency offset is the length of the radiating patch on the superstrate being 0.957 mm long instead of the designed 0.98 mm. In the measurement a matching better than 10 dB is achieved in an absolute bandwidth of about 9 GHz corresponding to a relative bandwidth of 11%. This means a degradation of 4% in comparison to the simulated fractional bandwidth.

The gain measurement was performed with a 20 dBi E-band standard gain horn antenna mounted 0.59 m above the chuck of the probe station as demonstrated in Fig. 4. The gain was calculated with the procedure of [12] with a comparative measurement to a 10 dBi standard gain horn antenna. The insertion loss and the reflections at the probe were deembedded and the resulting gain of the integrated antenna is presented in Fig. 6. Additionally, the specified and measured values of the standard gain horn antenna are indicated in Fig. 6 to serve as a reference for the measurement accuracy. Above 70 GHz the measured gain of the standard gain horn antenna is permanently below the specified values of its data sheet denoting a slightly too low gain in the resulting curves. The

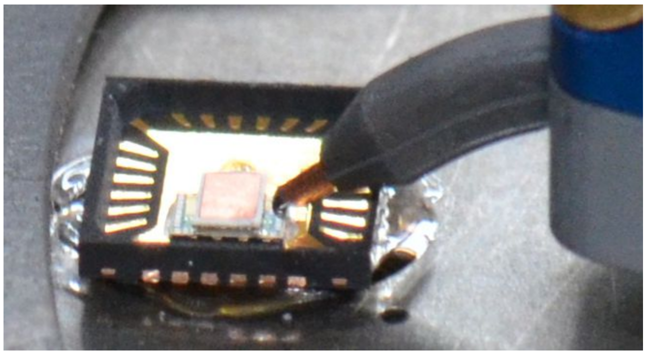

Fig. 7: Chip with integrated antenna and contacted probe tip.

ripple on the measurement curves are caused by multipath scattering. Under the 10 dBi standard gain horn reference antenna the chuck of the probe station could be completely covered with absorbing material. For the measurement of the AUT with the probe tip the full shielding of the chuck was not possible anymore. This could be a reason why the ripple on the curve of the AUT is higher than that of the reference antenna. The measured maximum gain to broadside of about 2 dBi differs by 2 dB from the simulated value of 4 dBi. Reasons for this discrepancy could be a lower efficiency of the antenna or a tilt of the main beam due to the probe tip in the near field of the radiating patch depicted in Fig. 7. In case of a pure degradation of the efficiency, this would mean a reduction from the simulated value of 50% to about 30% in the measurement. Due to the distance of 100 µm from the probe to dielectric plate with the radiating patch a tilt of the main beam is probable. Consequently, the assumed value of 30% is a kind of lower bound for the peak efficiency. The issue of probing in the near field of the integrated antenna cannot be investigated with this setup. For this reason a new antenna measurement setup containing an industrial robot to move the receiving horn antenna above the probe station is under construction [13].

B. *Determination of Radiation Pattern*

The second part of the antenna characterization was employed in an anechoic chamber. The radiation pattern can be measured in two ways. As shown in Fig. 1, the antenna on

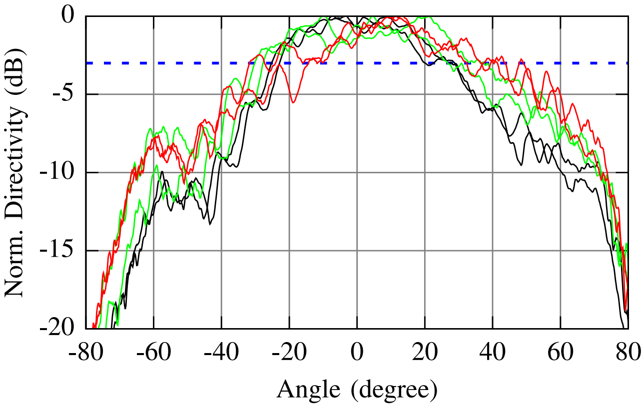

(a) H-plane.

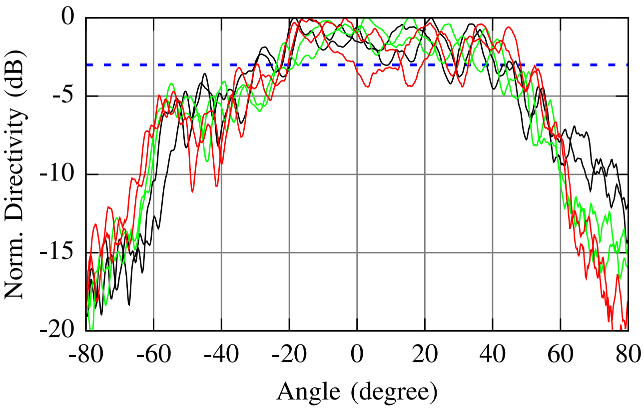

(b) E-plane.

Fig. 8: Normalized directivity for the frequencies 74 GHz and 76 GHz (—), 78 GHz and 80 GHz (—), 82 GHz and 84 GHz (—), and a −3 dB orientation line (- - -).

chip can be fed by the multiplier and amplifier acting as a transmit antenna, or as a receiving antenna with the LNA and the mixer to baseband. The integrated antenna was used in the transmitting mode because the leakage of the LO signal of the mixer on the chip to the LNA would downgrade the sensitivity in the receiving mode. The radiation pattern could only be measured with relative values due to the unknown amplifier output power and the unknown insertion loss of the transmit / receive coupler. The normalized directivity of the integrated antenna was measured for six frequencies between 74 GHz and 84 GHz. The radiation pattern in H- and E-plane of the packaged chip in the QFN package on a PCB are given in Fig. 8 for the mentioned frequencies. The considered angle range is between $-80°$ and $80°$ because the absorbing material at the edges of the PCB mask the direct line of sight to the receiving horn antenna for larger angles. The integrated antenna shows a wide directional characteristic in the E- and H-plane with no strong notches at any angle in the frequency band from 74 GHz to 84 GHz. The 3 dB beamwidth of the radiation pattern is about $55° - 65°$ in the H-plane and about $60° - 70°$ in the E-plane. The ripples are probably induced by superposition of radiation from the patch antenna and radiated surface waves at the edges of the QFN exposed pad. The isolation of the cross polarization is better than 10 dB and thus lower than the isolation of common patch antennas. A reason for this are the bond wires and also the huge radiating patch element overlapping one chip edge. These circuit parts produce parasitic stray fields causing a higher cross polarization level.

VI. Conclusion

An integrated antenna on an FMCW radar chip was presented with two independent characterization procedures. In a first measurement scenario with probe tips the gain and matching of the integrated antenna could be determined. The antenna is matched better than 10 dB between 75 GHz and 84 GHz and has a gain of 2 dBi to broadside corresponding to an efficiency of about 30%. The different measurement options are created by use of the FIB process and a short-circuited $\lambda/4$ transformer parallel to the antenna feeding structure.

References

[1] B. Heinemann, R. Barth, D. Bolze, J. Drews, G. Fischer, A. Fox, O. Fursenko, T. Grabolla, U. Haak, D. Knoll, R. Kurps, M. Lisker, S. Marschmeyer, H. Rücker, D. Schmidt, J. Schmidt, M. Schubert, B. Tillack, C. Wipf, D. Wolansky, and Y. Yamamoto, "SiGe HBT technology with f_T/f_{max} of 300 GHz/500 GHz and 2.0 ps CML gate delay," in *2010 IEEE International Electron Devices Meeting (IEDM)*, December 2010, pp. 30.5.1–30.5.4.

[2] Rücker, H. and Heinemann, B., "SiGe BiCMOS technology for mm-wave systems," in *2012 International SoC Design Conference (ISOCC)*, November 2012, pp. 266–268.

[3] I. Sarkas, S. Nicolson, A. Tomkins, E. Laskin, P. Chevalier, B. Sautreuil, and S. Voinigescu, "An 18-Gb/s Direct QPSK Modulation SiGe BiCMOS Transceiver for Last Mile Links in the 70–80 GHz Band," *IEEE Journal of Solid-State Circuits*, vol. 45, no. 10, pp. 1968–1980, October 2010.

[4] M. Girma, S. Beer, J. Hasch, M. Gonser, W. Debski, W. Winkler, Y. Sun, and T. Zwick, "Miniaturized 122 GHz system-in-package (SiP) short range radar sensor," in *2013 European Radar Conference (EuRAD)*, October 2013, pp. 49–52.

[5] R. Wang, Y. Sun, M. Kaynak, S. Beer, J. Borngraber, and J. Christoph Scheytt, "A micromachined double-dipole antenna for 122–140 GHz applications based on a SiGe BiCMOS technology," in *2012 IEEE MTT-S International Microwave Symposium Digest (MTT)*, June 2012, pp. 1–3.

[6] D. Hou, Y.-Z. Xiong, W.-L. Goh, S. Hu, W. Hong, and M. Madihian, "130-GHz On-Chip Meander Slot Antennas With Stacked Dielectric Resonators in Standard CMOS Technology," *IEEE Transactions on Antennas and Propagation*, vol. 60, no. 9, pp. 4102–4109, September 2012.

[7] R. Alhalabi and G. Rebeiz, "Design of high-efficiency millimeter-wave microstrip antennas for silicon RFIC applications," in *Antennas and Propagation (APSURSI), 2011 IEEE International Symposium on*, July 2011, pp. 2055–2058.

[8] Y.-C. Ou and G. Rebeiz, "Differential Microstrip and Slot-Ring Antennas for Millimeter-Wave Silicon Systems," *IEEE Transactions on Antennas and Propagation*, vol. 60, no. 6, pp. 2611–2619, June 2012.

[9] J. Hasch, U. Wostradowski, S. Gaier, and T. Hansen, "77 GHz radar transceiver with dual integrated antenna elements," in *German Microwave Conference, 2010*, March 2010, pp. 280–283.

[10] Rogers Corporation, Rogers, CT 06263, USA.

[11] IHP, Frankfurt (Oder) 15236, Germany.

[12] H. Gulan, S. Beer, S. Diebold, C. Rusch, A. Leuther, I. Kallfass, and T. Zwick, "Probe based antenna measurements up to 325 GHz for upcoming millimeter-wave applications," in *2013 International Workshop on Antenna Technology (iWAT)*, March 2013, pp. 228–231.

[13] M. Hitzler, S. Bader, and C. Waldschmidt, "Key Aspects of Robot based Antenna Measurements at Millimeter Wave Frequencies, accepted for publication at the EuCAP 2014," in *2014 8th European Conference on Antennas and Propagation (EuCAP)*, April 2014.